Queen Mary
University of London

Tuning the energetics and tailoring the optical properties of silver clusters confined in zeolites.

Fenwick, O; Coutiño-Gonzalez, E; Grandjean, D; Baekelant, W; Richard, F; Bonacchi, S; De Vos, D; Lievens, P; Roeffaers, M; Hofkens, J; Samorì, P

For additional information about this publication click this link.
http://qmro.qmul.ac.uk/xmlui/handle/123456789/13014

Space confinement of silver clusters in zeolites: Tuning the energetics and tailoring exceptional optical properties

Oliver Fenwick[1], Eduardo Coutiño-Gonzalez[2], Wouter Baekelant[2], Fanny Richard[1], Sara Bonacchi[1], Maarten Roeffaers[3]*, Johan Hofkens[2]*, Paolo Samorì[1]*

[1] *ISIS & icFRC, Université de Strasbourg & CNRS, 8, allée Gaspard Monge, 67000 Strasbourg, France. E-mail : samori@unistra.fr*

[2] *Department of Chemistry, KULeuven, Celestijnenlaan 200F, B-3001 Leuven, Belgium. E-mail: Johan.Hofkens@chem.kuleuven.be*

[3] *Department of of Microbial and Molecular Systems, KULeuven, Kasteelpark Arenberg 23, B-3001 Leuven, Belgium. E-mail: Maarten.Roeffaers@biw.kuleuven.be*

The unique properties acquired by matter when confined in space represent a hallmark of nanosciences and nanotechnology. The integration of metal atoms and clusters in well-defined dielectric cavities is a powerful strategy to impart novel properties to them that depend on both the size and geometry of the confined space as well as on the electrostatic interaction between the metal and the local host environment. Here, for the first time, we unravel the dependence of the electronic properties of metal clusters on space confinement by studying the ionisation potential of silver clusters embedded in four different zeolite environments over a range of silver concentrations. The combination of optical and photoelectron spectroscopy investigations reveals a strong influence of the silver loading and the host environment on the cluster ionisation potential, which is also correlated to the optical properties. Through fine-tuning of the zeolite host environment and silver concentration, we demonstrate photoluminescence quantum yields approaching unity.

MAIN TEXT

Self-assembly is a well-established approach to build-up 1, 2 or 3 dimensional hierarchical structures with controlled organisation at distinct length scales. It is therefore an ideal method to guide both the chemical and physical properties of a system, surpassing the scope of properties that can be obtained in conventional liquid or solid-state environments. A particularly interesting method to direct the self-assembly process is the use of confined spaces such as pores, channels or cages which impose restrictions on the final geometry and dimensions of an embedded functional self-assembled system.
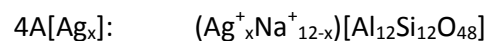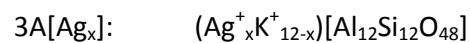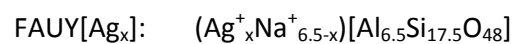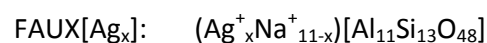
Small noble metal clusters can exhibit molecule-like behaviour in terms of their electronic transitions, and certain clusters of silver atoms have proved particularly interesting due to their pronounced catalytic[1], antimicrobial[2] and optical properties.[3] However, the difficulty in obtaining samples with monodisperse cluster sizes and their tendency to aggregate makes harnessing these exciting properties for applications challenging.[4] To circumvent this problem, a number of stabilising strategies have been proposed including soft matter approaches based on DNA,[3,5] polyphosphates,[6,7] organic polymers[8] and peptides,[9] and more rigid approaches relying on glasses[10,11] and zeolites.[12-15] Zeolites are readily available as naturally occurring minerals, but can also be synthesised in industrial quantities at low cost with a tailored structure and tunable porosity. They are attractive as hosts for silver clusters because of the relative ease with which Ag^+ ions can be incorporated by means of ion exchange, as well as their well-defined crystal structures with cages and channels of molecular dimensions which can influence the geometry and nuclearity of the clusters. Furthermore, the tunable combination of the overall negative framework charge, the coordinating properties of the lattice oxygen atoms and the counter-cations all work to stabilise clusters of certain sizes and geometries. The wealth of different framework

topologies and chemical compositions, and the variety of possible counter-cations in extra-framework positions makes silver-exchanged zeolites a highly versatile system in which a variety of luminescent clusters can be assembled with emission spanning much of the visible spectrum and with photoluminescence yields reported of up to 67 %.[12] This has made them attractive as next-generation secondary emitters in fluorescent lamps[16] and as wavelength converting materials in solar cells.[17]

In advancing the state-of-the-art for Ag cluster-containing zeolites for fluorescence applications it is mandatory to learn how to master the versatility of their chemistry to fully exploit the properties that emerge due to space confinement, i.e. emission wavelength and photoluminescence quantum yield (PLQY). Autoreduction processes have been identified in the formation of silver clusters in zeolites by calcination, with the required electrons originating from the expulsion of oxygen atoms from the zeolite framework or from the oxidation of hydration water to oxygen. However, despite much effort, relatively little is known about how to control the nuclearity and location of the clusters within zeolite hosts. Moreover, the relationship between the electronic and structural properties of such minuscule metal structures and their luminescence features has not been fully understood. In this paper we systematically study the effect of space confinement on Ag clusters formed inside zeolitic hosts. In particular, we explore the role of a) the framework topology, b) the degree of silver exchange, c) the negative framework charge density of the zeolite host, and d) the cationic species in the parent zeolite. With control over these four key parameters we correlate the optical properties with the ionisation potentials of the silver clusters, and ultimately tune the emission from the green to deep red, demonstrating PLQYs of close to 100 %.

We focussed our attention on two prototypical framework topologies which are used as hosts of luminescent silver clusters, Linde type A (LTA) and faujasite (FAU) (Figure 1 a). Both contain sodalite cages, but differ in the secondary building units interconnecting these cages. Luminescent Ag_3^{n+} clusters are the most frequently reported in FAU frameworks,[18-22] whilst both Ag_3^{n+} and Ag_6^{n+} clusters are frequently identified in LTA frameworks.[22,23] There are limited reports of other clusters forming, including Ag_4^{n+} in LTA frameworks[15] and Ag_2^{n+}, Ag_4^{n+} and Ag_8^{n+} in FAU frameworks.[21,24,25] The two faujasite frameworks chosen for this study, FAUX and FAUY, differ in the Si/Al ratio of the framework (1.2 for FAUX and 2.7 for FAUY from data provided by the suppliers) enabling us to explore the role of framework charge. The two LTA zeolites, 3A and 4A, differ in the alkali metal charge-balancing cation of the parent material, with the Na^+-containing 4A zeolite having an effective pore size of 4 Å, and the larger K^+ cations in the 3A zeolite restricting the effective pore size to 3 Å.

Starting from the parent zeolites, silver exchange was carried out in an aqueous silver nitrate solution before calcination at 450 °C in air to allow cluster formation (full procedure in the Methods section). We obtained fully- and partially-exchanged zeolites which we refer to according to their silver content relative to the dehydrated unit cells normalised to 24 T-atoms (the tetrahedrally coordinated Si and Al atoms):

FAUX[Ag_x]: $(Ag_x^+ Na_{11-x}^+)[Al_{11}Si_{13}O_{48}]$

FAUY[Ag_x]: $(Ag_x^+ Na_{6.5-x}^+)[Al_{6.5}Si_{17.5}O_{48}]$

3A[Ag_x]: $(Ag_x^+ K_{12-x}^+)[Al_{12}Si_{12}O_{48}]$

4A[Ag_x]: $(Ag_x^+ Na_{12-x}^+)[Al_{12}Si_{12}O_{48}]$

The composition of the calcined zeolites was verified by XPS (Supplementary Figure 8), confirming that the zeolites are in fully dehydrated form and allowing us to map step-by-step the progressive silver loading. The ratios of silver to alkali metal at intermediate exchange levels were slightly different from the ratios supposed from the exchange solution concentrations (Supplementary Figure 9), which may be due to inhomogeneous depth distribution of the charge balancing cations noting that XPS is a surface sensitive technique.[26] Nonetheless, for the sake of simplicity, our nomenclature will refer to the amount of silver calculated from the concentrations of the starting solutions. A small amount of sodium was detected in the 3A[Ag_0] unexchanged zeolite (i.e. alkali metal composition is 15 % Na and 85 % K as a proportion of the ion exchange capacity:). XPS shows that this sodium impurity was exchanged approximately in line with the proportion of K^+ exchanged. Na and K were detected by XPS in 3A at all silver loadings including in nominally fully exchanged 3A[Ag_{12}], but could be removed by using an excess of silver in the exchange solution (Supplementary Figure 10). To characterise the bonding environment of silver, we followed the Auger spectra of the calcined zeolite. The Auger electrons are ejected in a three electron process, and as such are highly sensitive to the chemical bonding of the element. We calculated the modified Auger parameters (MAPs) which are equal in this case to the sum of the binding energy of $3d_{5/2}$ electrons and the kinetic energy of $M_4N_{4,5}N_{4,5}$ Auger electrons and quantify the shift of atomic orbitals due to their chemical environment without susceptibility to charging effects.[27] The MAPs of silver clusters in the zeolites amount to 721.9 ± 0.4 eV for 3A[Ag_x], 722.2 ± 0.4 eV for FAUX[Ag_x], and 723.3 ± 0.4 eV for FAUY[Ag_x] which represent a very large chemical shift (3 - 5 eV) compared to silver metal (MAP = 726.0 eV) and a 1 − 2 eV chemical shift compared to silver (I) oxide (MAP = 724.1 eV). These chemical shifts are indicative of small Ag clusters.[28] Larger silver

nanoparticles have been detected by XPS in other zeolite frameworks,[29] but in our zeolites, we can rule out the presence of even small quantities of silver nanoparticles both from the large chemical shift and from the absence of metallic features in the Auger spectrum that are observed for nanoparticles (Figure 1 b).

We used photoelectron spectroscopy in air (PESA) for the first time to quantify the ionisation potentials (IPs) of metal clusters in well-defined confined spaces; these measurements were done on powder samples. Our results provide unambiguous evidence of a pronounced silver loading effect (Figure 2a), with the ionisation potentials gradually increasing with the silver content by up to 0.5 eV, as well as evidence of an influence of the zeolitic host. In determining the origin of the silver loading effect, one must consider that silver-exchanged zeolites are bimetallic systems (excluding the framework aluminium) with both silver and alkali metal cations/clusters present in the zeolite. The decrease of the IP with decreasing silver loading is due to the effect of the reduced photoelectron signal coming from silver clusters combined with an increased signal from alkali metal (Na, K) ions (or clusters[30,31], Supplementary Figures 6 and 7). This shifts the measured IP (Supplementary Figure 5) towards the value of the latter, noting that the IPs of sodium and potassium clusters[32-35] and metals[36] are known to be lower than those of silver.

In order to study the effect of the framework type, we focussed our attention on fully exchanged zeolites where silver is the only extra-framework metal. It is clear that the IPs in the four zeolitic hosts are markedly different, with the FAU frameworks having larger IPs than LTA (FAUY[$Ag_{6.5}$] the largest being 5.45 eV and the smallest being 5.16 eV obtained with 3A[Ag_{12}]). These results clearly demonstrate that the self-assembly of silver clusters in the confined space of the zeolites is strongly affected both by the geometry and the charge

density of the environment as well as the density of silver in the framework ($6.45/nm^3$ for fully loaded 3A and 4A zeolites versus $6.10/nm^3$ for FAUX[Ag_{13}] and $3.60/nm^3$ for FAUY[$Ag_{6.5}$]).

Excitation-emission spectra of the LTA zeolites (Figure 3 b) show the emergence of new bathochromically shifted peaks at progressively higher silver loading suggesting the formation of larger clusters. On the other hand, FAU zeolites show a remarkable resilience to larger cluster formation across the full range of silver loadings as ascertained both from the lack of emergence of new peaks in the excitation-emission spectra at high silver loadings (Supplementary Figures 1 and 2) and from the hypsochromic spectral shift with respect to clusters in the LTA frameworks. It is therefore reasonable that the IPs of the clusters in fully-loaded 3A and 4A zeolites are lower than for those in FAUX and FAUY since the HOMO levels of silver clusters are known to increase with increasing nuclearity.[37] Ag_3^{n+} clusters have IPs of 5.6 - 5.7 $eV^{[38-41]}$ for $n = 0$ (computed values[38,41] and from photoelectron spectroscopy on clusters in noble gas droplets[39,40]), so the clusters in the zeolite cavities clearly have slightly lower ionisation potentials either due to a different cluster geometry induced by the interaction with the zeolite framework or to an electronic interaction of the clusters with the lattice oxygen atoms.

Analysis of the relationship between the IPs of the fully loaded zeolites and the peak emission energy of the clusters (Figure 2 b), reveals that an increase in the IP is accompanied by a corresponding increase in the emission energy. In particular, a straight-line fit to this data yields a gradient close to two (1.8 ± 0.3), with the implication that the about half of the framework-induced shift in emission energy is due to a shift in the HOMO

level of the luminescent clusters and about half is due to an equal magnitude shift of their LUMO in the opposite direction.

The fully exchanged zeolites 3A[Ag_{12}] and 4A[Ag_{12}] have nominally identical compositions but quite different excitation-emission spectra (Figure 3a). The charge-balancing cations in the starting material, K^+ and Na^+ respectively, occupy the same extra-framework sites and, though they are exchanged with Ag^+ in a different order due to the non-equivalence of those sites,[42] fully exchanged 3A[Ag_{12}] and 4A[Ag_{12}] should be identical materials. In our case, XPS analysis reveals residual quantities of Na^+ and K^+ in 3A[Ag_{12}] amounting to 15 % of the total metal ions present (Supplementary Figure 10). Such unexchanged ions will impact on cluster formation and are responsible for the spectral differences between 3A[Ag_{12}] and 4A[Ag_{12}]. To confirm this, we carried out ion exchange in an excess of silver nitrate. XPS analysis confirms the complete elimination of K^+ ions in 3A[Ag_{excess}] and of the remaining metal cations <1% were Na^+, thus confirming >99 % silver exchange (Supplementary Figure 10). As a result, the photoluminescence properties of 3A[Ag_{excess}] and 4A[Ag_{excess}] (Figure 4) are strikingly similar with a single strong emission in the red, confirming the important role played by small residual counter-cation concentrations in silver cluster formation.

On the other hand, FAUX and FAUY frameworks differ in their dielectric environment because of their different Si/Al ratios whilst sharing the same topology. Our previous studies revealed that higher PLQYs can be obtained by exploiting the FAU topology rather than LTA, due to the preferential formation of photo-absorbing but non-emissive species in LTA zeolites.[12] These species are probably Ag^+ ions that have not formed clusters, since we can rule out the role of other extra-framework cations (Na^+, K^+) from diffuse reflectance spectra which indicate that they are not involved in absorption. It is therefore very interesting to

observe the PLQYs of the silver clusters in these FAUX and FAUY zeolites, which, although

similar at higher silver loadings (40-60% for *[Ag$_x$] x ≥ 3*), deviate significantly at lower

loadings. For the FAUX zeolite, the PLQY increases from 1 % at *x = 1* before reaching a

plateau at *x ≈ 5*, whilst for FAUY the PLQY at the lowest loading (*x = 0.5*) is 97.4 ± 2.1 % and

decreases to a plateau at higher silver concentrations. The PLQY in FAUY[Ag$_{0.5}$] is by far the

highest quantum yield observed for any silver species contained in zeolite frameworks[12] and

also exceeds the best quantum yields of silver clusters stabilised in other materials. [3,5,43,44]

Consequently, this result is an important milestone in the development of these materials as

secondary emitters for lighting and bio-imaging[44] applications, bringing the performance of

metal cluster-containing zeolites up to that of certain dye-containing zeolites[45].

Furthermore achievement of these high efficiencies at low silver concentrations inside the

rigid zeolite framework makes them cost-effective and also reduces potential concerns over

toxicity.

Whilst all silver atoms in FAUY[Ag$_{0.5}$] efficiently form highly luminescent clusters during the

calcination treatment, this is not the case when FAUX[Ag$_1$] is employed. In the later case

non-luminescent silver ions compete for the photon absorption resulting in a strongly

reduced PLQY. The absence of emerging peaks in the excitation-emission spectra at higher

silver loading indicates that the type of luminescent cluster formed in FAUX and FAUY

zeolites is not dependent on silver loading, and therefore that cluster formation at low silver

loading seems to be hindered in FAUX. In fact, the difference in electrostatic environments

inside the FAU frameworks is known to result in a larger activation energy for Na$^+$ migration

in FAUY compared to FAUX[46-48], but a lower activation energy for silver in FAUY compared to

FAUX[49]. Consequently, Ag$^+$ ions are more mobile than Na$^+$ ions in FAUY, but the opposite is

true for FAUX[49]. The reason for this counterintuitive trend in ionic conduction is the trade-off between the Coulombic framework-cation interaction, which diminishes for larger ionic radii, and cation-cation repulsion which increases with ionic radius and is more prominent in FAUX zeolites than FAUY due to the higher cation density[49]. The upshot of this is that silver cluster formation should be favoured in FAUY, even at low loadings, but it is inhibited in FAUX where a significant silver concentration threshold must be exceeded before luminescent clusters will form. At high silver loadings, there is probably a saturation of the sites for cluster formation and hence an increase in the population of silver in other sites where it is active in optical absorption but not emission. As a result the PLQY is less than 100 % for both FAUX and FAUY in this regime.

In this work we have shown that the rigid frameworks of zeolites provide a surprisingly versatile host for the stabilisation of silver clusters, and enable a high degree of control over their optoelectronic properties, which we have characterised with optical and photoelectron spectroscopy techniques. In particular, the degree of silver loading in the framework and the framework type allow the possibility to tune the ionisation potential over a range of >0.5 eV, which we can also correlate with the optical properties. Metal clusters are known to aggregate in the solid state with low quantum yields as a result, yet we have shown that, with the use of zeolite hosts, photoluminescence quantum yields can be optimised by varying the degree of silver loading and framework type whilst also considering the ionic mobilities of the non-framework metal cations in the zeolite. In this way we were able to produce silver cluster-containing FAUY zeolites with unity quantum yield, exceeding all previous reports on silver clusters and marking an important milestone

in the development of these materials for technological applications such as next-generation secondary emitters in fluorescent lamps. This work therefore establishes the use of rigid confined spaces with tunable topological and electrostatic properties as a powerful method to direct self-assembly and achieve enhanced material properties not accessible by other means.

METHODS

Synthesis of luminescent silver exchanged zeolites.

Synthesis of the silver-exchanged zeolites was carried out starting from 500 mg of the zeolite material (3A zeolite with Si/Al = 1; 4A zeolite with Si/Al = 1; FAUX zeolite with Si/Al = 1.2 from UOP; and FAUY zeolite with Si/Al = 2.7 from ZEOLYST). The zeolite powder was suspended in 500 mL of an aqueous silver nitrate solution containing the desired weight percentage (0.04 - to 0.5 mM, Sigma-Aldrich, 99% purity), the suspension was agitated overnight in the dark using an end-over-end shaker. The powder was recovered by filtration using a Büchner filter and washed several times with deionised water, then the sample was calcined overnight at 450 °C (5 °C/minute) following 2 steps of 15 minutes each at 100 and 150 °C to prevent any damage in the zeolite structure. After calcination the samples were cooled and stored in the dark for its further analysis.

Steady-state luminescence characterization.

For the emission-excitation characterisation, the calcined Ag containing zeolite samples were placed in a quartz cuvette (1 mm path length) and sealed by a Teflon stopper. Emission

and excitation spectra were recorded using an Edinburgh Instruments FLS 980 fluorimeter (corrected for wavelength dependence throughput and sensitivity of the detection channel). For every excitation wavelength, the emission was collected starting 30 nm above the excitation wavelength and ending at 800 nm using 5 nm steps. The signal above 410 nm was measured using a 400 nm long pass glass filter to avoid interference from second-order excitation peaks, the measured intensities were corrected for the transmittance of the long pass filter. The emission was collected in "front face mode" through the quartz cuvette and sent to a PMT for detection. From the separate emission spectra at varying excitation wavelengths, the two dimensional excitation-emission matrices were constructed, the raw data was corrected for background and noise and interpolated to a resolution of 1 nm x 1 nm.

Photoluminescence quantum yield measurement.

Absolute photoluminescence yields were measured using an integrating sphere[12] (Labsphere optical Spectralon integrating sphere, 100 mm diameter) coupled to a fluorimeter (Edinburgh Instruments FLS 980) through optical fibers (in Supplementary Figure 3 a schematic representation of the set-up is shown). The sphere accessories were made from Teflon (sample holder). Two commercial phosphors ($BaMgAl_{10}O_{19}:Eu^{2+}$, and $BaMgAl_{10}O_{19}:Eu^{2+},Mn^{2+}$) with known PLQY were measured and used as references for the calibration of the set-up. [50]

Photoelectron spectroscopy in air (PESA)

The ionisation potentials of the silver-exchanged zeolites were determined by photoelectron spectroscopy in air (PESA) using a Riken Keiki spectrophotometer (Japan) model AC-2. A substrate of evaporated gold on glass was used with the zeolite powder

gently compressed on top to form a flat surface of coverage > 1cm^2. The conditions

employed during the measurements were a scanning energy range from 4.3 to 6.2 eV with a

measurement interval of 0.05 eV, an integration time of 100 s and UV spot intensity of 1500

nW.

X-ray phototoelectron spectroscopy (XPS)

X-ray photoelectron spectroscopy was performed on the silver-exchanged zeolite powders

with a Thermo Scientific™ K-Alpha™ X-ray Photoelectron Spectrometer (XPS) System. The

AlKα source produces x-rays (*hv = 1486.7 eV)* that are focussed to a 200 x 200 μm spot

(power density = 66 W/m^2). Both Ag3d$_{5/2}$ spectra and Ag Auger spectra were measured with

a pass-energy of 50 eV and step of 0.1 eV. An electron flood gun was applied during the XPS

measurements to minimize charging effects.

REFERENCES

1   Martens, J. A. *et al.* NOx abatement in exhaust from lean-burn combustion engines by reduction of NO2 over silver-containing zeolite catalysts. *Angew. Chem. Int. Ed.* **37**, 1901-1903 (1998).
2   Lalueza, P., Monzón, M., Arruebo, M. & Santamaría, J. Bactericidal effects of different silver-containing materials. *Mater. Res. Bull.* **46**, 2070-2076 (2011).
3   Vosch, T. *et al.* Strongly emissive individual DNA-encapsulated Ag nanoclusters as single-molecule fluorophores. *Proc. Natl. Acad. Sci. U. S. A.* **104**, 12616-12621 (2007).
4   Dubertret, B. *et al.* In Vivo Imaging of Quantum Dots Encapsulated in Phospholipid Micelles. *Science* **298**, 1759-1762 (2002).
5   Richards, C. I. *et al.* Oligonucleotide-stabilized Ag nanocluster fluorophores. *J. Am. Chem. Soc.* **130**, 5038-5039 (2008).
6   Henglein, A. Small-particle research - Physicochemical properties of extremely small colloidal metal and semiconductor particles. *Chem. Rev.* **89**, 1861-1873 (1989).
7   Mulvaney, P. & Henglein, A. Long-lived nonmetallic silver clusters in aqueous solution - a pulse-radiolysis study of their formation. *J. Phys. Chem.* **94**, 4182-4188 (1990).
8   Diez, I. *et al.* Blue, green and red emissive silver nanoclusters formed in organic solvents. *Nanoscale* **4**, 4434-4437 (2012).
9   Yu, J., Patel, S. A. & Dickson, R. M. In vitro and intracellular production of peptide-encapsulated fluorescent silver nanoclusters. *Angew. Chem.* **119**, 2074-2076 (2007).

10   Borsella, E. *et al.* Synthesis of silver clusters in silica-based glasses for optoelectronics applications. *J. Non-Cryst. Solids* **245**, 122-128 (1999).

11   Shestakov, M. V. *et al.* Lead silicate glass SiO_2-PbF_2 doped with luminescent Ag nanoclusters of a fixed site. *RSC Adv.* **4**, 20699-20703 (2014).

12   Coutino-Gonzalez, E. *et al.* Determination and optimization of the luminescence external quantum efficiency of silver-clusters zeolite composites. *J. Phys. Chem. C* **117**, 6998-7004 (2013).

13   Grobet, P. J. & Schoonheydt, R. A. ESR on silver clusters in zeolite A. *Surf. Sci.* **156**, 893-898 (1985).

14   Seifert, R., Kunzmann, A. & Calzaferri, G. The yellow color of silver-containing zeolite A. *Angew. Chem. Int. Ed.* **37**, 1521-1524 (1998).

15   Wasowicz, T. & Michalik, J. Reactions of silver atoms and clusters in Ag-NaA zeolites. *Radiat. Phys. Chem* **37**, 427-432 (1991).

16   Vosch, T. *et al.* Emissive lamps comprising metal clusters confined in molecular sieves. BE2008/00050 (WO2009006707) (2009).

17   Pandey, L. *et al.* Solar Cells. BE2008/00051 (WO2009006708 A3) (2009).

18   De Cremer, G. *et al.* In situ observation of the emission characteristics of zeolite-hosted silver species during heat treatment. *ChemPhysChem* **11**, 1627-1631 (2010).

19   Gellens, L. R., Mortier, W. J., Lissillour, R. & Lebeuze, A. Electronic-structure of the silver clusters in zeolites of type A and the faujasite type by molecular-orbital calculations. *J. Phys. Chem.* **86**, 2509-2516 (1982).

20   Gellens, L. R., Mortier, W. J., Schoonheydt, R. A. & Uytterhoeven, J. B. The nature of the charged silver clusters in dehydrated zeolites of type A. *J. Phys. Chem.* **85**, 2783-2788 (1981).

21   Gellens, L. R., Mortier, W. J. & Uytterhoeven, J. B. On the nature of the charged silver clusters in zeolites of type A, type X and type Y. *Zeolites* **1**, 11-18 (1981).

22   Sun, T. & Seff, K. Silver clusters and chemistry in zeolites. *Chem. Rev.* **94**, 857-870 (1994).

23   Mayoral, A., Carey, T., Anderson, P. A., Lubk, A. & Diaz, I. Atomic resolution analysis of silver ion-exchanged zeolite A. *Angew. Chem. Int. Ed.* **50**, 11230-11233 (2011).

24   Kim, S. Y., Kim, Y. & Seff, K. Two crystal structures of fully dehydrated, fully Ag+-exchanged zeolite X. Dehydration in oxygen prevents Ag+ reduction. Without oxygen, Ag-8(n+) (T-d) and cyclo-Ag-4(m+) (near S-4) form. *J. Phys. Chem. B* **107**, 6938-6945 (2003).

25   Lee, S. H., Kim, Y. & Seff, K. Weak Ag+–Ag+ bonding in zeolite X. Crystal structures of Ag92Si100Al92O384 hydrated and fully dehydrated in flowing oxygen. *Microporous Mesoporous Mater.* **41**, 49-59 (2000).

26   Fibikar, S., Rinke, M. T., Schäfer, A. & Cola, L. D. Quantification of cation-exchanged zeolites by XPS and EDS: A comparative study. *Microporous Mesoporous Mater.* **132**, 296-299 (2010).

27   Gaarenstroom, S. W. & Winograd, N. Initial and final-state effects in ESCA spectra of Cadmium and silver oxides. *J. Chem. Phys.* **67**, 3500-3506 (1977).

28   Fonseca, A. M. & Neves, I. C. Study of silver species stabilized in different microporous zeolites. *Microporous Mesoporous Mater.* **181**, 83-87 (2013).

29   Anson, A., Maham, Y., Lin, C. C. H., Kuznicki, T. M. & Kuznicki, S. M. XPS characterization of silver exchanged ETS-10 and mordenite molecular sieves. *J. Nanosci. Nanotechnol.* **9**, 3134-3137 (2009).

30   Blake, N. & Stucky, G. Alkali-metal clusters as prototypes for electron solvation in zeolites. *J. Incl. Phenom. Macrocycl. Chem.* **21**, 299-324 (1995).

31   Kasai, P. H. Electron spin resonance studies of γ- and X-ray-irradiated zeolites. *J. Chem. Phys.* **43**, 3322-3327 (1965).

32   Foster, P. J., Leckenby, R. E. & Robbins, E. J. The ionization potentials of clustered alkali metal atoms. *J. Phys. B* **2**, 478-483 (1969).

33   Honea, E. C., Homer, M. L., Persson, J. L. & Whetten, R. L. Generation and photoionization of cold Na_n clusters - n to 200. *Chem. Phys. Lett.* **171**, 147-154 (1990).

34 Onwuagba, B. N. Ionization potentials in alkali-metal clusters. *Il Nuovo Cimento D* **13**, 415-421 (1991).

35 Martins, J. L., Buttet, J. & Car, R. Equilibrium geometries and electronic-structures of small sodium clusters. *Phys. Rev. Lett.* **53**, 655-658 (1984).

36 Kaye, G. W. C. & Laby, T. H. *Tables of physical and chemical constants*. 16th edn, (1995).

37 Jackschath, C., Rabin, I. & Schulze, W. Electron impact ionization of silver clusters Ag_n, $n \leqq 36$. *Z. Phys. D: At., Mol. Clusters* **22**, 517-520 (1992).

38 Huang, M.-J. & Watts, J. D. Theoretical study of triatomic silver (Ag_3) and its ions with coupled-cluster methods and correlation-consistent basis sets. *Phys. Chem. Chem. Phys.* **14**, 6849-6855 (2012).

39 Przystawik, A. *et al.* Photoelectron studies of neutral Ag_3 in helium droplets. *J. Chem. Phys.* **126**, 184306 (2007).

40 Alameddin, G., Hunter, J., Cameron, D. & Kappes, M. M. Electronic and geometric structure in silver clusters. *Chem. Phys. Lett.* **192**, 122-128 (1992).

41 Tian, D., Zhang, H. & Zhao, J. Structure and structural evolution of Ag_n (n=3-22) clusters using a genetic algorithm and density functional theory method. *Solid State Commun.* **144**, 174-179 (2007).

42 Meyer, M., Leiggener, C. & Calzaferri, G. Particle distribution in a microporous material: Experiments with zeolite A. *ChemPhysChem* **6**, 1071-1080 (2005).

43 Kuznetsov, A. S., Tikhomirov, V. K., Shestakov, M. V. & Moshchalkov, V. V. Ag nanocluster functionalized glasses for efficient photonic conversion in light sources, solar cells and flexible screen monitors. *Nanoscale* **5**, 10065-10075 (2013).

44 Choi, S., Dickson, R. M. & Yu, J. H. Developing luminescent silver nanodots for biological applications. *Chem. Soc. Rev.* **41**, 1867-1891 (2012).

45 Devaux, A. *et al.* Self-absorption and luminescence quantum yields of dye-zeolite L composites. *J. Phys. Chem. C* **117**, 23034-23047 (2013).

46 Mortier, W. J. & Schoonheydt, R. A. Surface and solid-state chemistry of zeolites. *Prog. Solid State Chem.* **16**, 1-125 (1985).

47 Freeman, D. C. & Stamires, D. N. Electrical conductivity of synthetic crystalline zeolites. *J. Chem. Phys.* **35**, 799-806 (1961).

48 Simon, U. & Franke, M. E. Electrical properties of nanoscaled host/guest compounds. *Microporous Mesoporous Mater.* **41**, 1-36 (2000).

49 Kalogeras, I. M. & Vassilikou-Dova, A. Electrical properties of zeolitic catalysts. *Defect Diffus. Forum* **164**, 1-36 (1998).

50 Leyre, S. *et al.* Absolute determination of photoluminescence quantum efficiency using an integrating sphere setup. *Rev. Sci. Instrum.* **85**, 23115-23115 (2014).

AUTHOR CONTRIBUTIONS

PS and JH conceived the experiments. OF, FR and SB conducted the photoelectron spectroscopy experiments. ECG and WB prepared the Ag-zeolites and conducted the optical characterisation. OF and PS prepared the manuscript with contributions from all co-authors.
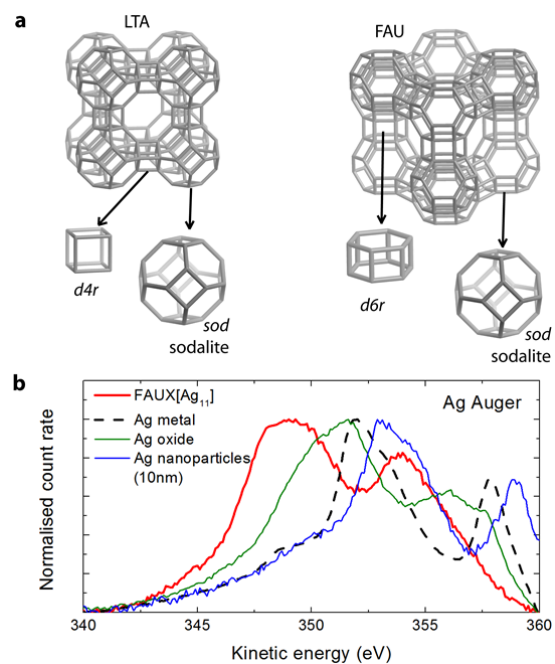
Figure 1 – **Topology of the zeolite frameworks and Auger spectra of their silver clusters. a** Schematic of the LTA and FAU zeolite frameworks and their building blocks. Vertices of the stick model indicate T-atom (Al or Si) positions. For clarity oxygen atoms and the counter-cations are not shown. **b** Auger spectra of silver in four forms: metallic, Ag(I) oxide, 10 nm sodium citrate stabilised nanoparticles, and as clusters in a calcined zeolite (FAUX[Ag$_{11}$]).
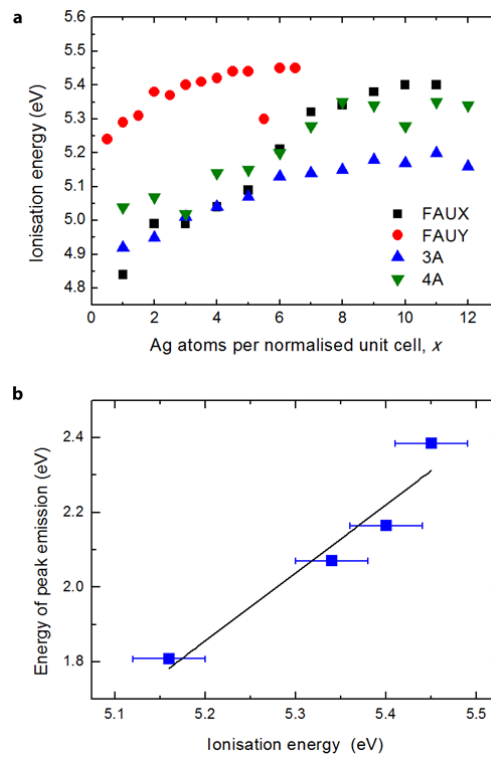
Figure 2 Ionisation potentials of the heat-treated silver-exchanged zeolites a Ionisation potentials of the four calcined zeolites (FAUX, FAUY, 3A and 4A) across the full range of silver loadings determined from PESA measurements. **b** Peak emission energy plotted against ionisation potential for the four fully-exchanged zeolites (FAUX[Ag_{11}], FAUY[$Ag_{6.5}$], 3A[Ag_{12}] and 4A[Ag_{12}]).
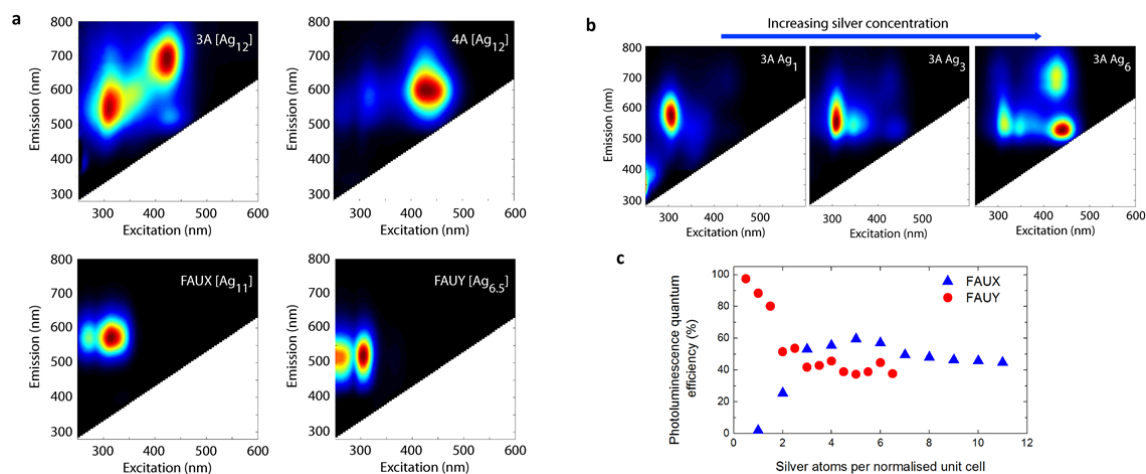
Figure 3 – Photoluminescence properties of heat-treated silver-exchanged zeolites. a Excitation-emission two-dimensional plots of the fully exchanged and calcined zeolites of the four frameworks studied (3A, 4A, FAUX and FAUY). **b** Excitation-emission two-dimensional plots of the 3A zeolite at intermediate silver loadings showing the growth of new peaks with increasing silver loading. **c** Photoluminescence quantum yields (λ_{exc} = 305 nm) of the FAU zeolites across the full range of silver loadings showing significant deviation between the FAUX and FAUY zeolites at low silver concentrations.
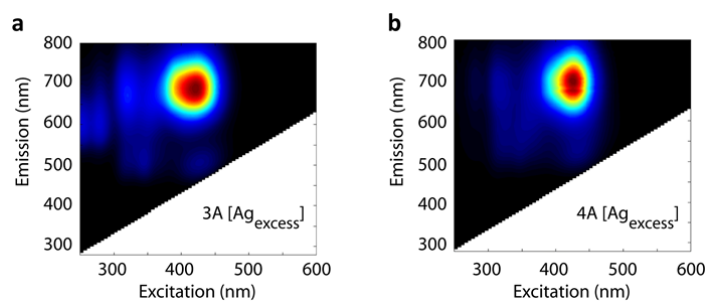

Figure 4 – Photoluminescence properties of calcined 3A and 4A zeolites where ion-exchange was performed in a solution with excess silver ions. Excitation-emission two-dimensional plots of the fully exchanged and calcined zeolites where exchange was performed with an excess concentration of silver nitrate, 3A[Ag$_{excess}$] and 4A[Ag$_{excess}$]. It can be seen that under these conditions, where all Na$^+$ and K$^+$ ions have been exchanged, the spectra of the two are similar.